Geometric Modelling of the Human Cornea: A New Approach for the Study of Corneal Ectatic Disease. A Pilot Investigation

Francisco Cavas-Martínez[1(✉)], Daniel G. Fernández-Pacheco[1], Dolores Parras[1], Francisco J.F. Cañavate[1], Laurent Bataille[2], and Jorge L. Alio[3,4,5]

[1] Department of Graphical Expression, Technical University of Cartagena, Cartagena, Spain
{francisco.cavas, daniel.garcia, dolores.parras, francisco.canavate}@upct.es
[2] Research and Development Department, Vissum Corporation, Alicante, Spain
lbataille@vissum.com
[3] Division of Ophthalmology, Universidad Miguel Hernández, Alicante, Spain
jlalio@vissum.com
[4] Keratoconus Unit of Vissum Corporation, Alicante, Spain
[5] Department of Refractive Surgery, Vissum Corporation, Alicante, Spain

Abstract. Purpose: The aim of this study was to describe the application of a new bioengineering graphical technique based on geometric custom modelling capable to detect and to discriminate small variations in the morphology of the corneal surface.

Methods: A virtual 3D solid custom model of the cornea was obtained employing Computer Aided Geometric Design tools, using raw data from a discrete and finite set of spatial points representative of both sides of the corneal surface provided by a corneal topographer. Geometric reconstruction was performed using B-Spline functions, defining and calculating the representative geometric variables of the corneal morphology of patients under clinical diagnosis of keratoconus.

Results: At least four variables could be used in order to classify corneal abnormalities related to keratoconus disease: anterior corneal surface area (ROC 0.853; $p < 0.0001$), posterior corneal surface area (ROC 0.813; $p < 0.0001$), anterior apex deviation (ROC 0.742; $p < 0.0001$) and posterior apex deviation (ROC 0.899; $p < 0.0001$).

Conclusions: Custom geometric modelling enables an accurate characterization of the human cornea based on untreated raw data from the corneal topographer and the calculation of morphological variables of the cornea, which permits the clinical diagnosis of keratoconus disease.

Keywords: Keratoconus · CAD · Scheimpflug · Surface reconstruction · Virtual model

I. Rojas and F. Ortuño (Eds.): IWBBIO 2017, Part I, LNBI 10208, pp. 271–281, 2017.
DOI: 10.1007/978-3-319-56148-6_23

1 Introduction

The analysis of the geometric characteristics of the cornea has been of interest in ophthalmology given that small variations in its morphology can suppose important changes in visual function of the patient [1]. Thus, the geometric reconstruction of the corneal surface has experienced significant progress in recent years with the development of new technologies [2]. This reconstruction process is currently being developed by the so-called modal methods, based mainly on the development of the Zernike polynomials. However, this approach has limitations as it is inaccurate in abnormal situations: eyes after corneal surgery or eyes with corneal pathology (such as keratoconus) that present significant higher-order aberrations [3–6].

An alternative to these surface reconstruction methods are the zonal methods, mainly based on B-splines, which are stable geometric reconstruction mathematical functions [7, 8]. However, these methods have not been widely used in ophthalmology.

On the other hand, over recent years the development of new computational tools has improved the process of acquisition and image processing [9], enabling to generate three-dimensional shapes [10] and to develop behavioral models which reproduce the geometry of a solid structure more accurately.

One of these tools is the Computer Aided Geometric Design (CAGD), which was created to address the technological needs of companies in automotive and aeronautic sectors. The CAGD allows to study the geometric and computational aspects of any complex physical entity such as areas and volumes to create virtual models [11], which differentiate from physical models for not having a destructive process and reducing costs in terms of production and time [12, 13].

Specifically in the field of Bioengineering, the development of virtual models through CAGD permits the characterization of biological structures, establishing new experimentation procedures in the field of medicine [14]. The development of these three-dimensional models of biological structures [15] allows to optimize the design of prosthesis [16], to perform biomechanical studies using finite elements [17], to obtain virtual representations for educational purposes [18], or simply to generate realistic physical models from a virtual model using 3D printing techniques [19].

Based on all of the above and applied to the field of ophthalmology, this study proposes a new technique for the clinical diagnosis of corneal ectatic diseases. This is a bioengineering graphical technique based on the performance of an integral geometric analysis of a 3D representative model of the corneal structure of a live patient, where the model obtained presents a high sensitivity to small variations that may occur in the morphology of both anterior and posterior corneal surfaces. This accurate characterization of the human cornea enables a new path in the diagnosis of this corneal ectatic disease and offers a new approach that facilitates the follow-up of keratoconus.

2 Materials and Methods

The retrospective study adhered to the tenets of the Declaration of Helsinki and was approved by the local Clinical Research Ethics Committee of Vissum Corporation (Alicante, Spain). Patients examined at the Vissum Corporation (Alicante, Spain) were

retrospectively enrolled. Patients were selected from a database of candidates for refractive surgery with normal corneas [20, 21] and also a database of cases diagnosed with keratoconus [20, 21] in both eyes.

All eyes selected (187) underwent a thorough and comprehensive eye and vision examination which included [20, 21] uncorrected distance visual acuity (UDVA), corrected distance visual acuity (CDVA), manifest refraction, Goldmann tonometry, biometry (IOLMaster, Carl Zeiss Meditec AG) and corneal topographic analysis. During this protocol, the Sirius system® (CSO, Florence, Italy) was used, which is a noninvasive system for measuring and characterizing the anterior segment using a rotating Scheimpflug camera that generates images in three dimensions, with a dot matrix fine-meshed in the center due to the rotation. The images taken during the examination are digitalized in the main unit and transferred to a computer and analyzed in detail. Gathered Sirius corneal topographies (data from other topographers such as Pentacam can also be handled [22]) are represented as discrete and finite set of spatial points (point cloud surfaces) in the form of two 31×256 matrices. Both matrices contain the polar coordinates representative of the anterior and posterior corneal surfaces. These data, used only in the first stage of the topographic data acquisition procedure, are called raw data [4, 23]. This warrantied that data were not interpolated or manipulated [22, 23], avoiding any proprietary reconstruction software from topographer's manufacturer. All measurements were performed by the same experienced optometrists, performing three consecutive measurements and taking average values for posterior analysis.

2.1 Diagnosis Procedure

The technique proposed in this article, based on zonal methods, has two well differentiated stages: a first stage where a 3D model of the cornea is reconstructed from the raw data provided by the corneal topographer using CAGD tools, and a second stage where several geometric variables are extracted from the model and analyzed to characterize the cornea.

First Stage: 3D Model Reconstruction
The reconstruction process can be divided into four phases (Fig. 1):

1. Extraction of the point clouds from the Sirius topographer.
2. Generation of both corneal surfaces. The two point clouds were imported to the surface reconstruction CAD software Rhinoceros® V 5.0 (MCNeel & Associates, Seattle, USA). This software provides useful functions, such as B-splines, to generate surfaces with high accuracy. For this study the Rhinoceros' patch surface function was used, obtaining a mean distance error between the 3D point cloud and the solution surface of about $3.60 \times 10^{-4} \pm 6.43 \times 10^{-4}$ mm.
3. Positioning of both corneal surfaces. After the generation of both corneal surfaces, they were engaged by their geometrical center and Z axis.
4. Reconstruction of the 3D model. Once both corneal surfaces were positioned, the peripheral surface (the bonding surface between both sides in the Z-axis direction) was generated and all surfaces were then joined to form a single surface. The surface reconstructed was then exported to the solid modeling software SolidWorks V 2013

(Dassault Systèmes, Vélizy-Villacoublay, France) to generate a 3D model representative of the custom and actual geometry of the cornea.

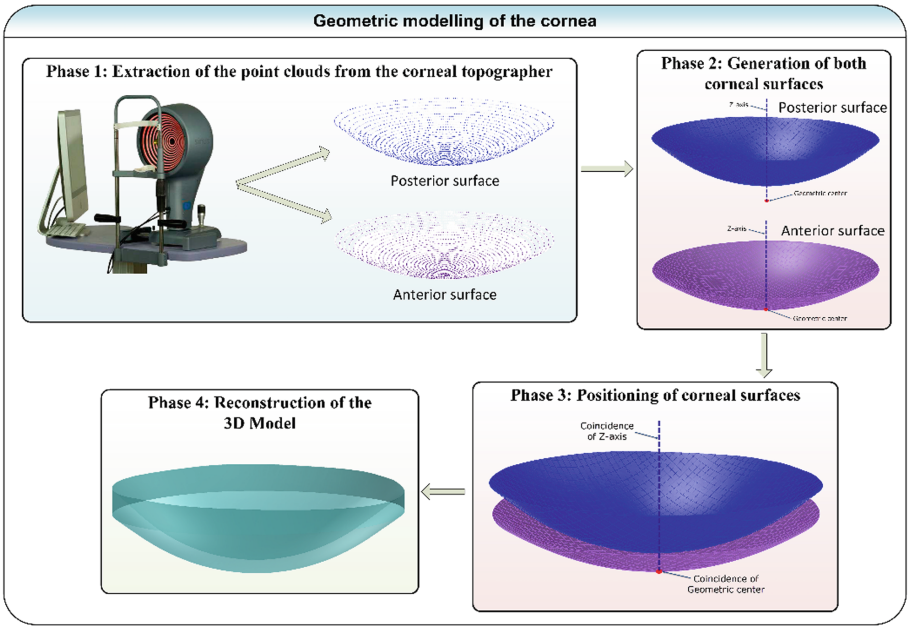

Fig. 1. Geometric modelling process by using DGAO tools.

Second Stage: Characterization of the Cornea

During this stage, some geometric variables representative of the corneal morphology were calculated from the 3D model generated on the previous stage. A detailed description of the geometric variables used during this study can be found in Table 1.

These variables were later statistically analyzed in order to characterize the cornea.

Table 1. Geometric variables analyzed in the study.

Geometric variable	Description
Total corneal volume [mm3]	Volume limited by front, back and peripheral surfaces of the solid model generated
Anterior corneal surface area [mm2]	Area of the front/exterior surface
Posterior corneal surface area [mm2]	Area of the rear/interior surface
Total corneal surface area [mm2]	Sum of anterior, posterior and perimetral corneal surface areas of the solid model generated
Anterior apex deviation [mm]	Average distance from the Z axis to the highest point (apex) of the anterior corneal surfaces
Posterior apex deviation [mm]	Average distance from the Z axis to the highest point (apex) of the posterior corneal surfaces

2.2 Statistical Analysis

A Kolmogorov-Smirnov test was run to assess the data engagement scores. According to this test and thereafter, a Student's t-test or U-Mann Whitney Wilcoxon test was performed (depending on normality), in order to describe differences between normal and keratoconus groups in all the measurements proposed. Additionally, Kruskal Wallis (K-W) and Effect Size (ES) tests were used to compare differences and to quantify the degree of change between groups according to Amsler Krumeich Grading System (AK). ROC curves were established to determine what parameters could be used to classify the diseased corneas by calculating optimal cut-offs, sensitivity and specificity. All the analyses were performed by using Graphpad Prism v6 (GraphPad Software, La Jolla, USA) and SPSS v17.0 software (SPSS, Chicago, USA).

3 Results

From a total of 187 patients, this study included 124 healthy eyes that did not present any ocular pathology [20] and constituted by 69 females (55.6%) and 55 males (44.4%) ranged from 7 to 73 years old, and 63 eyes diagnosed with keratoconus in several grades [21] (53.9% in stage I, 31.7% in stage II, and 14.4% in the most extreme stages, III and IV) and formed by 34 females (53.9%) and 29 males (46.1%) ranged from 14 to 69 years old.

All of the modeled variables showed differences between normal and keratoconic eyes, as seen in Table 2. Total corneal volume presents higher values in healthy eyes ($p < 0.0001$), while anterior and posterior corneal surface areas are lower in the same subjects ($p < 0.0001$). This pattern of difference can be seen for most of the variables studied: healthy corneas have anterior and posterior apex deviations lower than keratoconic corneas ($p < 0.0001$).

Outcomes according to keratoconus severity are shown in Table 3, where comparisons are established according to the AK grading system. Additionally, note that

Table 2. Variables measured in healthy and keratoconic corneas, Mean ± SD (range)

Morphogeometric parameters	Healthy N = 124	Keratoconic N = 63	
	Mean ± SD (range)	Mean ± SD (range)	p value (statistical test)
Total corneal volume [mm^3]	25.90 ± 0.31 (25.59 to 26.21)	23.51 ± 0.48 (23.03 to 23.99)	0.0001 Mann-Whitney
Anterior corneal surface area [mm^2]	43.13 ± 0.06 (43.07 to 43.19)	43.42 ± 0.13 (43.29 to 43.55)	0.0001 Mann-Whitney
Posterior corneal surface area [mm^2]	44.31 ± 0.09 (44.22 to 44.40)	44.81 ± 0.21 (44.6 to 45.02)	0.0001 Mann-Whitney
Total corneal surface area [mm^2]	104.02 ± 0.29 (103.73 to 104.31)	103.68 ± 0.43 (103.25 to 104.11)	0.0001 Mann-Whitney
Anterior apex deviation [mm]	0.0003 ± 0.0002 (0.0001 to 0.0005)	0.0090 ± 0.0035 (0.0055 to 0.0125)	0.0001 Mann-Whitney
Posterior apex deviation [mm]	0.0771 ± 0.0128 (0.0643 to 0.0899)	0.1902 ± 0.029 (0.1603 to 0.2201)	0.0001 Mann-Whitney

Table 3. Variables measured in healthy and keratoconic corneas, Mean ± SD (range)

	Normal	Stage I	Stage II	Stage III-IV	p (KW test)
Total corneal volume [mm^3]	25.90 ± 0.31 (25.59 to 26.21)	23.51 ± 0.48 (23.03 to 23.99)	23.09 ± 0.59 (22.5 to 23.68)	20.01 ± 2.88 (17.13 to 22.89)	0.0001
(ES)	–	1.21	1.39	3.41	
Anterior corneal surface area [mm^2]	43.13 ± 0.06 (43.07 to 43.19)	43.42 ± 0.13 (43.29 to 43.55)	43.50 ± 0.17 (43.33 to 43.67)	44.31 ± 0.21 (44.1 to 44.52)	0.0001
(ES)	–	−1.16	−1.66	−4.79	
Posterior corneal surface area [mm^2]	44.31 ± 0.09 (44.22 to 44.40)	44.81 ± 0.21 (44.6 to 45.02)	44.99 ± 0.22 (44.7 to 45.21)	45.39 ± 0.32 (45.07 to 45.71)	0.0001
(ES)	–	−0.101	−1.49	−4.21	
Total corneal surface area [mm^2]	104.02 ± 0.29 (103.73 to 104.31)	103.68 ± 0.43 (103.25 to 104.11)	103.59 ± 0.39 (103.2 to 103.98)	103.53 ± 0.52 (103.01 to 104.05)	0.0001
(ES)	–	0.31	0.20	0.29	
Anterior apex deviation [mm]	0.0001 ± 0.00001 (0.0000 to 0.0002)	0.006 ± 0.0021 (0.0039 to 0.0081)	0.009 ± 0.0035 (0.0055 to 0.0125)	0.012 ± 0.004 (0.008 to 0.016)	0.0001
(ES)	–	−1.11	−1.39	−5.70	
Posterior apex deviation [mm]	0.0771 ± 0.0128 (0.0643 to 0.0899)	0.17 ± 0.029 (0.141 to 0.199)	0.201 ± 0.03 (0.171 to 0.231)	0.237 ± 0.051 (0.186 to 0.288)	0.0001
(ES)	–	−1.19	−1.40	−1.23	

(ES): Effect size

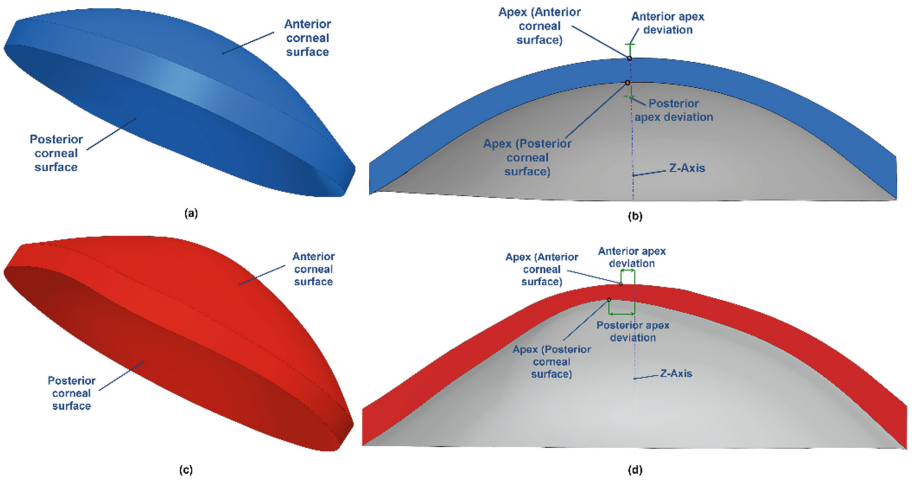

Fig. 2. Geometric variables analyzed during the study that achieved the best results: (a) 3D model of a healthy cornea, (b) Cut of a healthy cornea by a sagittal plane through the corneal apex, (c) 3D model of a diseased cornea, (d) Cut of a diseased cornea by a sagittal plane through the corneal apex.

calculated effect sizes for each disease stage allows quantifying the degree of change, higher for stages III and IV in all of the variables, becoming more evident with the progress of the disease.

The predictive value of the modeled variables was established by a ROC analysis (Fig. 3). From the several geometric variables analyzed during the study, the variables that achieved the best results in the diagnosis of the disease with an area under the ROC curve (AUROC) above 0.7 were the following four: *anterior corneal surface area* (Fig. 2) (area: 0.853, $p < 0.0001$, std. error: 0.040, 95% CI: 0.762–0.919), with a cutoff value of 43.07 mm^2, and an associated sensitivity and specificity of 90.27% and 60.01%, respectively; *the posterior corneal surface area* (Fig. 2) (area: 0.813, $p < 0.0001$, std. error: 0.039, 95% CI: 0.719–0.891), with a cutoff value of 44.18 mm^2, and an associated sensitivity and specificity of 91.08% and 44.17%, respectively; *anterior apex deviation* (Fig. 2) (area: 0.742, $p < 0.0001$, std. error: 0.059, 95% CI: 0.641–0.875), with a cutoff value of 0.0013 mm, and an associated sensitivity and specificity of 72.02% and 92.01%, respectively; *posterior apex deviation* (Fig. 2) (area:

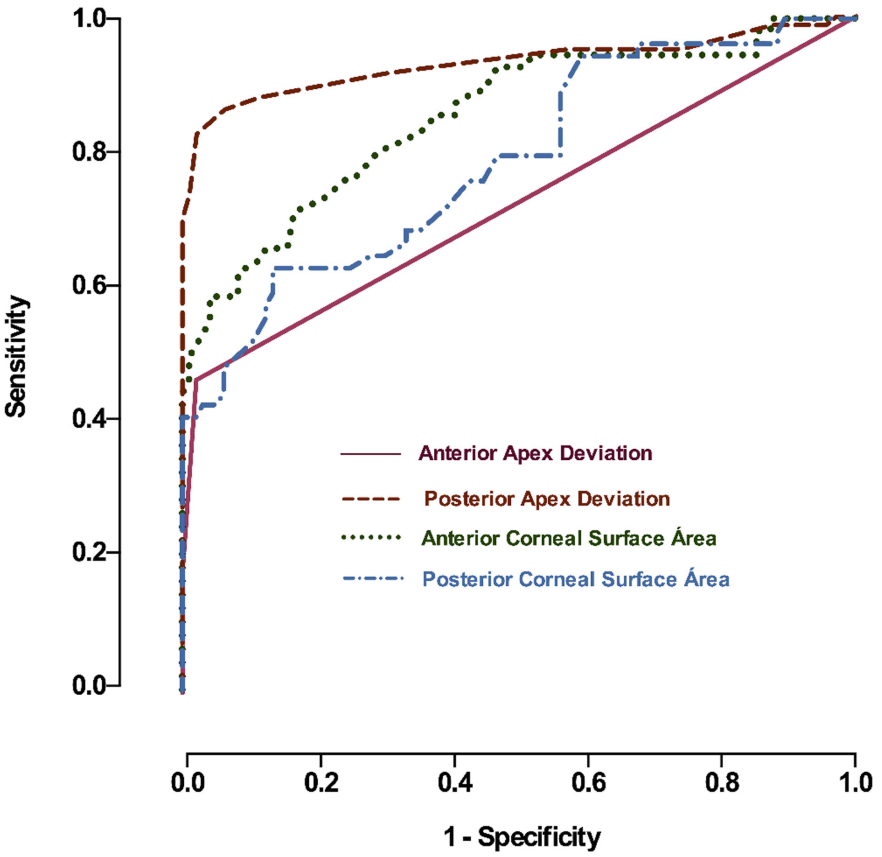

Fig. 3. A ROC analysis modelling the sensitivity versus 1-specificity for variables predicting the existence of keratoconus disease using geometrical custom modelling of the cornea

0.899, $p < 0.0001$, std. error: 0.041, 95% CI: 0.800–0.964), with a cutoff value of 0.0855 mm, and an associated sensitivity and specificity of 91.28% and 73.07%, respectively. Thus, according to the area under the curve variable calculated for the four variables, it was concluded that the parameter that provides a higher rate of discrimination between normal corneas and corneas with keratoconus is *Posterior apex deviation*. Nevertheless, there are other relevant statistical differences between healthy and diseased eyes, and most of variables studied differ between groups, making it possible to differentiate with high sensitivity and specificity healthy corneas from those patients diagnosed with keratoconus.

4 Discussion

This study has been carried out with the aim of assessing the ability of a specific geometric model to capture diseases on human corneas, accounting only for geometrical data. Specifically, this computational study provides insight into the complex clinical problem of diagnosing corneal ectatic diseases.

It is well known that the mechanical response of any deformable system is affected by its geometry and material properties. When geometry is fully characterized, it is possible to set up a geometric model of the system, which may be used to analyze the geometric response under original conditions. In this case, conditions are defined by the rupture of the geometric balance due to the existence of a biomechanical weakening, as happens in the keratoconus disease. Keratoconus is a disorder characterized by a progressive thinning of the cornea, which is physically presented in its structure as a protrusion or cone type focal curving that entails a redistribution of its pachymetry and some changes in the anatomical morphology of its surfaces.

To date, there are devices that analyze topographically both corneal surfaces and allow an in vivo characterization of curvature changes, corneal pachymetry, etc. These parameters are used in the diagnosis of the disease and therefore could provide a characterization of the underlying morphogeometric alteration. However, the geometrical characterization indices proposed by these devices are not easily compatible between different tomographers, generating confusion in the Ophthalmic Community [24–27].

Other option is the geometric characterization based on raw data, which has been previously used by some authors in the Corneal Biomechanics field [22, 28] and for diagnosis of corneal diseases [29]. However, these studies resort to data interpolation to obtain a specific model for each patient.

Geometric modeling based on raw data that has not been treated by any internal algorithm of the topographer enables an accurate clinical characterization of the human cornea basing on perfectly defined morphological variables in the field of graphic bioengineering.

Furthermore, this study relies on the use of a reduced number of geometrical parameters obtained from modelling tests of the cornea: anterior corneal surface area, posterior corneal surface area, anterior apex deviation and posterior apex deviation. These variables are sufficient to prove that the variability of the geometric response of human corneas is definitely related with disease diagnosis. This method is simplified

and more integrative than current diagnostic systems, which analyze separately the anterior and posterior surfaces of the cornea.

This observation has a quite relevant implication in view of the prediction of the response to refractive surgery, i.e. the knowledge of the sole geometry is enough to feed keratoconus diagnosis.

5 Conclusions

The main suggestion derived from this study is to give high priority to the development of non-invasive testing methods that are able to provide through inverse analysis the patient-specific parameters of a sufficiently realistic geometric model of the corneal morphology, which can be obtained with the aid of Computer Aided Geometric Design tools.

This method will allow improving the detection and effects of therapeutic methods used for keratoconus and other corneal ectatic diseases such as post-lasik ectasia. Early studies, currently under publication, have demonstrated the effectiveness of this approach in the early detection of subclinical keratoconus. In a close future, thanks to the analyses of the objective data related to the geometric effect of the intracorneal rings implanted, customized nomograms for the implantation of IntraCorneal Rings will be developed. Later, the analysis of the correlation between the geometric, visual, biomechanical and clinical effects of intracorneal implants in ectatic corneas will allow the development of new therapies and new concepts of corneal implants. The geometric modeling developed will also allow assessing more accurately the outcomes of the corneal crosslinking techniques and its effectiveness in slowing the development of keratoconus.

References

1. Pinero, D.P., Alio, J.L., Barraquer, R.I., Michael, R., Jimenez, R.: Corneal biomechanics, refraction, and corneal aberrometry in keratoconus: an integrated study. Invest. Ophthalmol. Vis. Sci. **51**, 1948–1955 (2010)
2. de Jong, T., Sheehan, M.T., Dubbelman, M., Koopmans, S.A., Jansonius, N.M.: Shape of the anterior cornea: comparison of height data from 4 corneal topographers. J. Cataract Refr. Surg. **39**, 1570–1580 (2013)
3. Klyce, S.D., Karon, M.D., Smolek, M.K.: Advantages and disadvantages of the Zernike expansion for representing wave aberration of the normal and aberrated eye. J. Refract. Surg. **20**, S537–S541 (2004)
4. Ramos-Lopez, D., Martinez-Finkelshtein, A., Castro-Luna, G.M., Pinero, D., Alio, J.L.: Placido-based indices of corneal irregularity. Optom. Vis. Sci. **88**, 1220–1231 (2011)
5. Trevino, J.P., Gómez-Correa, J.E., Iskander, D.R., Chávez-Cerda, S.: Zernike vs. Bessel circular functions in visual optics. Ophthal. Physl. Opt. **33**, 394–402 (2013)
6. Lenarduzzi, L.: Compression of corneal maps of curvature. Appl. Math. Comput. **252**, 77–87 (2015)

7. Ares, M., Royo, S.: Comparison of cubic B-spline and Zernike-fitting techniques in complex wavefront reconstruction. Appl. Opt. **45**, 6954–6964 (2006)
8. Gong, D.W., Chen, J.H., Yuan, C., Ge, R.K., Zhou, M.H.: A new method for reconstruction of corneal topography with Placido disk system. Adv. Mat. Res. **974**, 373–378 (2014)
9. Eklund, A., Dufort, P., Forsberg, D., LaConte, S.M.: Medical image processing on the GPU - past, present and future. Med. Image Anal. **17**, 1073–1094 (2013)
10. Sun, W., Darling, A., Starly, B., Nam, J.: Computer-aided tissue engineering: overview, scope and challenges. Biotechnol. Appl. Biochem. **39**, 29–47 (2004)
11. Farin, G.E., Hoschek, J., Kim, M.-S.: Handbook of Computer Aided Geometric Design. Elsevier, Amsterdam (2002)
12. Pottmann, H., Leopoldseder, S., Hofer, M., Steiner, T., Wang, W.: Industrial geometry: recent advances and applications in CAD. CAD Comput. Aided Des. **37**, 751–766 (2005)
13. Cui, J., Tang, M., Liu, H.: Dynamic shape representation for product modeling in conceptual design. Jisuanji Fuzhu Sheji Yu Tuxingxue Xuebao/J. Comput.-Aided Des. Comput. Graph. **26**, 1879–1885 (2014)
14. Lohfeld, S., Barron, V., McHugh, P.E.: Biomodels of bone: a review. Ann. Biomed. Eng. **33**, 1295–1311 (2005)
15. Almeida, H.A., Bártolo, P.J.: Computational technologies in tissue engineering. WIT Trans. Biomed. and Health **17**, 117–129 (2013)
16. Ovcharenko, E.A., Klyshnikov, K.U., Vlad, A.R., Sizova, I.N., Kokov, A.N., Nushtaev, D. V., Yuzhalin, A.E., Zhuravleva, I.U.: Computer-aided design of the human aortic root. Comput. Biol. Med. **54**, 109–115 (2014)
17. Chiang, I.-C., Shyh-Yuan, L., Ming-Chang, W., Sun, C.W., Jiang, C.P.: Finite element modelling of implant designs and cortical bone thickness on stress distribution in maxillary type IV bone. Comput. Methods Biomech. Biomed. Eng. **17**, 516–526 (2014)
18. Rocha, M., Pereira, J.P., De Castro, A.V.: 3D modeling mechanisms for educational resources in medical and health area. In: Proceedings of the 6th Iberian Conference on Information Systems and Technologies (CISTI 2011) (2011)
19. Schubert, C., van Langeveld, M.C., Donoso, L.A.: Innovations in 3D printing: a 3D overview from optics to organs. Br. J. Ophthalmol. **98**, 159–161 (2014)
20. Montalban, R., Alio, J.L., Javaloy, J., Pinero, D.P.: Correlation of anterior and posterior corneal shape in keratoconus. Cornea **32**, 916–921 (2013)
21. Montalban, R., Pinero, D.P., Javaloy, J., Alio, J.L.: Correlation of the corneal toricity between anterior and posterior corneal surfaces in the normal human eye. Cornea **32**, 791–798 (2013)
22. Ariza-Gracia, M.A., Zurita, J.F., Pinero, D.P., Rodriguez-Matas, J.F., Calvo, B.: Coupled biomechanical response of the cornea assessed by non-contact tonometry. Simulation study. PLoS One **10**, e0121486 (2015)
23. Cavas-Martinez, F., Fernandez-Pacheco, D.G., De la Cruz-Sanchez, E., Nieto Martinez, J., Fernandez Canavate, F.J., Vega-Estrada, A., Plaza-Puche, A.B., Alio, J.L.: Geometrical custom modeling of human cornea in vivo and its use for the diagnosis of corneal ectasia. PLoS ONE **9**, e110249 (2014)
24. Anayol, M.A., Guler, E., Yagci, R., Sekeroglu, M.A., Ylmazoglu, M., Trhs, H., Kulak, A.E., Ylmazbas, P.: Comparison of central corneal thickness, thinnest corneal thickness, anterior chamber depth, and simulated keratometry using galilei, Pentacam, and Sirius devices. Cornea **33**, 582–586 (2014)
25. Hernandez-Camarena, J.C., Chirinos-Saldana, P., Navas, A., Ramirez-Miranda, A., de la Mota, A., Jimenez-Corona, A., Graue-Hernindez, E.O.: Repeatability, reproducibility, and agreement between three different Scheimpflug systems in measuring corneal and anterior segment biometry. J. Refract. Surg. **30**, 616–621 (2014)

26. Savini, G., Carbonelli, M., Sbreglia, A., Barboni, P., Deluigi, G., Hoffer, K.J.: Comparison of anterior segment measurements by 3 Scheimpflug tomographers and 1 Placido corneal topographer. J. Cataract Refract. Surg. **37**, 1679–1685 (2011)
27. Shetty, R., Arora, V., Jayadev, C., Nuijts, R.M., Kumar, M., Puttaiah, N.K., Kummelil, M. K.: Repeatability and agreement of three Scheimpflug-based imaging systems for measuring anterior segment parameters in keratoconus. Invest. Ophthalmol. Vis. Sci. **55**, 5263–5268 (2014)
28. Simonini, I., Pandolfi, A.: Customized finite element modelling of the human cornea. PLoS ONE **10**, e0130426 (2015)
29. Ramos-Lopez, D., Martinez-Finkelshtein, A., Castro-Luna, G.M., Burguera-Gimenez, N., Vega-Estrada, A., Pinero, D., Alio, J.L.: Screening subclinical keratoconus with placido-based corneal indices. Optom. Vis. Sci. **90**, 335–343 (2013)